

Active control of the scattered radiation in the sound field with a reflected surface

Han, Ning¹

Key Laboratory of Underwater Acoustic Signal Processing of Ministry of Education
Southeast University, Nanjing 210096, China.

ABSTRACT

Active control systems were proposed in previous work for the three-dimension scattered radiation, where all the relevant simulations and experiments were implemented in three-dimensional free sound field. While for practical applications, the sound field conditions are usually complex, such as with reflected surfaces. It should be answered whether the previous control system is still effective in this condition, and furthermore what improvements should be operated to ensure the control effect. In the present research, based on the mirror image principle, a modified methods for calculating the control source strengths are proposed for the scattered radiation control in the sound field with a reflected surface, and the corresponding numerical simulations are implemented to detect the control effect. It is seen that the local active control is still effective with the improved methods of the scattered radiation control.

Keywords: Active control, scattered radiation, non-free sound field

I-INCE Classification of Subject Number: 38

1. INTRODUCTION

Active noise control (ANC) can be applied to reduce the scattered radiation from a scatterer impinged by an incident wave, which is useful for making objects such as submarines or underwater mines invisible to the active sonar systems.

In the free sound field, Senior [1] indicated that a wide degree of control over the scattering behavior of a spherical scatterer can be achieved by varying the loading impedance. With the piezoelectric material, Bao et al. [2–4] presented an active acoustic coating to prevent an incident sound wave from reflecting off the scatterer boundary submerged in a sound field, and Lafleur et al. [5, 6] formed an active surface to reduce the reflected or transmitted wave by single or double piezoelectric layers. An actuator–sensor tile, which contains a full area actuator, sound pressure and particle velocity sensors, was developed by Corsaro et al. [7] to control the reflection and transmission characteristics of the underwater structures actively. For the direct active control of the scattered wave, computing the control source strengths requires the knowledge of the scattered sound pressure, while in practice only the total sound pressure can be directly measured. Friot and Bordier [8, 9] introduced a method to distinguish the scattered wave from the total sound field through a layer of inner sensors and outer sensors, and then suppressed the scattered pressure by an active control system. Han et al. [10] proposed an approach for predicting the scattered sound pressure, and it is used in the error sensing strategy of the

control system to reduce the scattered radiation. Liu et al. [11] presented a control strategy that combines optimized loudspeaker arrays using constrained matching pursuit and zero pressure constrained points to control the scattered sound field of a rigid sphere.

However for practical applications, such as the anti-eavesdropping system or the stealth system for submarines, the sound field conditions are usually complex, and the most common case is the one with reflected surface. It is necessary to check the effectiveness of the previous control system in such condition or some improvements should be operated to ensure the control effect. In this paper, based on the mirror image principle, the control system for the scattered radiation is modelled in the sound field with an infinite reflected surface, and two methods are proposed for calculating the control source strengths. Simulations with one-channel (one control source and one error sensor) system are then implemented to detect the corresponding control effect, according to the two methods above.

¹ hanning@seu.edu.cn

2. THERETICAL ANALYSIS IN NON-FREE SOUND FIELD

2.1 Model of the active control system for scattered radiation

Similar to the active control system for the scattered radiation in free sound field [10], the one in the sound field with one infinite reflected surface are shown in the left part of Fig. 1, where N_0 inner sensors are located on the rigid scatterer surface for predicting the scattered pressure at the outer virtual error sensors, and N_c control sources are located between the inner sensors and the outer virtual error sensors. Due to the existence of the reflected surface and according to the mirror image principle, the acoustic image of the primary source and the control source array are shown in the right part of Fig. 1, which will influence the sound pressures at the inner sensors and the virtual error sensors. The reason of using the “virtual error sensor” is that the scattered sound pressure, which needs to be controlled, cannot be obtained directly by locating a physical sensor there, but calculated by a prediction method.

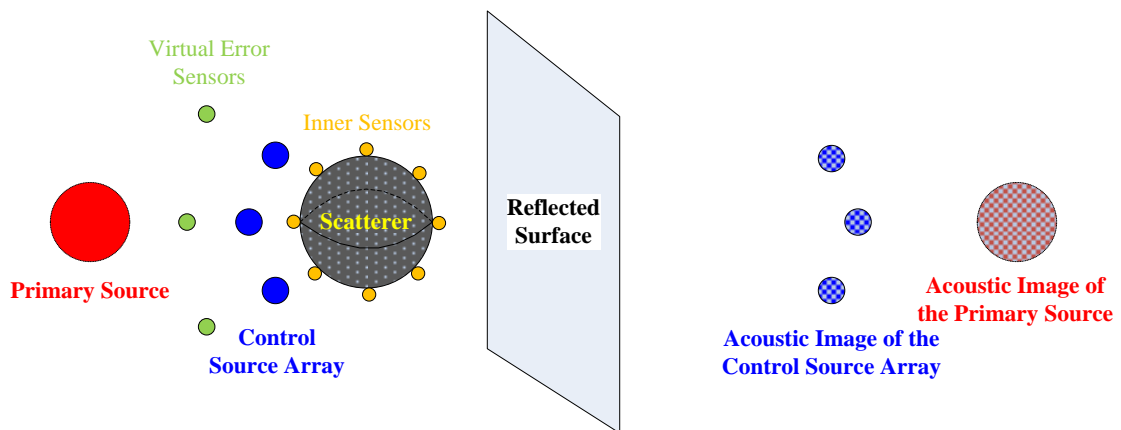


Fig. 1 Sketch-map of the active control system for the scattered radiation in non-free sound field

2.2 Active control of the scattered radiation

The sound pressure at N_e virtual error sensors $\mathbf{e}=[e_1 \ e_2 \ \cdots \ e_{N_e}]$ for the scattered radiation control is the sum of the scattered pressures \mathbf{p}_{ps} from the primary sources as well as \mathbf{p}_{pms} from their acoustic images, and the total (scattered and incident) pressures $\mathbf{p}_{cs} + \mathbf{p}_{ci}$ from the control sources as well as $\mathbf{p}_{cms} + \mathbf{p}_{cmi}$ from their acoustic images,

$$\mathbf{e} = \mathbf{p}_{ps} + \mathbf{p}_{pms} + \mathbf{p}_{cs} + \mathbf{p}_{cms} + \mathbf{p}_{ci} + \mathbf{p}_{cmi} \quad (1)$$

With the primary source strengths $\mathbf{Q}_p = [q_{p1} \ q_{p2} \ \cdots \ q_{pN_p}]^T$ and the control source strengths $\mathbf{Q}_c = [q_{c1} \ q_{c2} \ \cdots \ q_{cN_c}]^T$, \mathbf{Z}_{ps} is defined as a $N_e \times 2N_p$ matrix of the transfer functions between the scattered pressures at N_e error sensors and N_p primary sources as well as their N_p acoustic images, and \mathbf{Z}_c is defined as the $N_e \times 2N_c$ matrix of the transfer functions between the total (scattered and incident) pressures at N_e error sensors and N_c control sources as well as their N_c acoustic images. Then Eq. (1) is rewritten as

$$\mathbf{e} = \mathbf{Z}_{ps}[\mathbf{Q}_p; \mathbf{Q}_p] + \mathbf{Z}_c[\mathbf{Q}_c; \mathbf{Q}_c] \quad (2a)$$

$$\mathbf{Z}_{ps} = \begin{bmatrix} z_{ps(1,1)} & \cdots & z_{ps(1,N_p)} & z_{ps(1,N_p+1)} & \cdots & z_{ps(1,2N_p)} \\ \vdots & \ddots & \vdots & \vdots & \ddots & \vdots \\ z_{ps(N_e,1)} & \cdots & z_{ps(N_e,N_p)} & z_{ps(N_e,N_p+1)} & \cdots & z_{ps(N_e,2N_p)} \end{bmatrix} \quad (2b)$$

$$\mathbf{Z}_c = \begin{bmatrix} z_{c(1,1)} & \cdots & z_{c(1,N_c)} & z_{c(1,N_c+1)} & \cdots & z_{c(1,2N_c)} \\ \vdots & \ddots & \vdots & \vdots & \ddots & \vdots \\ z_{c(N_e,1)} & \cdots & z_{c(N_e,N_c)} & z_{c(N_e,N_c+1)} & \cdots & z_{c(N_e,2N_c)} \end{bmatrix} \quad (2c)$$

If $F = \sum_{n=1}^{N_e} \frac{1}{2\rho_0 c^2} e_n^2$ is defined as the cost function, which is minimized under the influence of the primary and control sources, the optimum control source strengths are obtained as [12]

$$\mathbf{Q}_{copt} = -\frac{1}{2} \mathbf{a}^{-1} (\mathbf{b}_1^H + \mathbf{b}_2) \quad (3)$$

where $\mathbf{a} = \frac{1}{2\rho_0 c^2} \mathbf{Z}_c^H \mathbf{Z}_c$, $\mathbf{b}_1 = \frac{1}{2\rho_0 c^2} [\mathbf{Q}_p; \mathbf{Q}_p]^H \mathbf{Z}_{ps}^H \mathbf{Z}_c$ and $\mathbf{b}_2 = \frac{1}{2\rho_0 c^2} \mathbf{Z}_c^H \mathbf{Z}_{ps} [\mathbf{Q}_p; \mathbf{Q}_p]$.

It is known that the control sources and their acoustic images must have the same source strengths, in that way, the strengths of N_c control sources are chosen to be the first half elements in \mathbf{Q}_{copt} , which is called Method 1.

On the other hand, with the transformations of \mathbf{Z}_{ps} and \mathbf{Z}_c , $\tilde{\mathbf{Z}}_{ps}$ and $\tilde{\mathbf{Z}}_c$ are defined to be a $N_e \times N_p$ matrix and a $N_e \times N_c$ matrix, respectively

$$\tilde{\mathbf{Z}}_{ps} = \begin{bmatrix} z_{ps(1,1)} & \cdots & z_{ps(1,N_p)} \\ \vdots & \ddots & \vdots \\ z_{ps(N_e,1)} & \cdots & z_{ps(N_e,N_p)} \end{bmatrix} + \begin{bmatrix} z_{ps(1,N_p+1)} & \cdots & z_{ps(1,2N_p)} \\ \vdots & \ddots & \vdots \\ z_{ps(N_e,N_p+1)} & \cdots & z_{ps(N_e,2N_p)} \end{bmatrix} \quad (4a)$$

$$\tilde{\mathbf{Z}}_c = \begin{bmatrix} z_{c(1,1)} & \cdots & z_{c(1,N_c)} \\ \vdots & \ddots & \vdots \\ z_{c(N_e,1)} & \cdots & z_{c(N_e,N_c)} \end{bmatrix} + \begin{bmatrix} z_{c(1,N_c+1)} & \cdots & z_{c(1,2N_c)} \\ \vdots & \ddots & \vdots \\ z_{c(N_e,N_c+1)} & \cdots & z_{c(N_e,2N_c)} \end{bmatrix} \quad (4b)$$

Therefore, Eq. (2a) can be simplified to be

$$\mathbf{e} = \tilde{\mathbf{Z}}_{ps} \mathbf{Q}_p + \tilde{\mathbf{Z}}_c \mathbf{Q}_c \quad (5)$$

The optimum strengths for N_c control sources are also calculated by Eq. (3), but with

$$\mathbf{a} = \frac{1}{2\rho_0 c^2} \tilde{\mathbf{Z}}_c^H \tilde{\mathbf{Z}}_c, \quad \mathbf{b}_1 = \frac{1}{2\rho_0 c^2} \mathbf{Q}_p^H \tilde{\mathbf{Z}}_{ps}^H \tilde{\mathbf{Z}}_c \quad \text{and} \quad \mathbf{b}_2 = \frac{1}{2\rho_0 c^2} \tilde{\mathbf{Z}}_c^H \tilde{\mathbf{Z}}_{ps} \mathbf{Q}_p, \quad \text{which is Method 2.}$$

3. NUMERICAL SIMULATIONS IN NON-FREE SOUND FIELD

In the numerical simulations of the control process, the scattered sound pressures at the error sensors are predicted through measuring the sound pressures $p(\bar{r}_0)$ on the scatterer surface, as in Ref. [10], where 20 inner sensors are used; while the scattered sound pressures before and after control will be calculated through the theoretical formulas [13], in order to evaluate the control effect strictly.

3.1 Scattered radiation control with one-channel control system

For practical applications, such as the stealth system preventing the submarines from being detected by active sonars, the main control area is usually in the source direction, therefore our attention is mainly paid on the local control. In the simulation model, one virtual error sensor and one control source, i.e., the one-channel control system is applied, and the relative locations to the source and the scatterer with 0.18m radius are shown in Fig. 2, where the infinite reflected surface has 0.5 reflection coefficient.

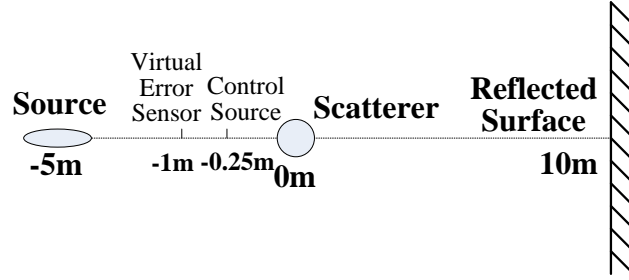
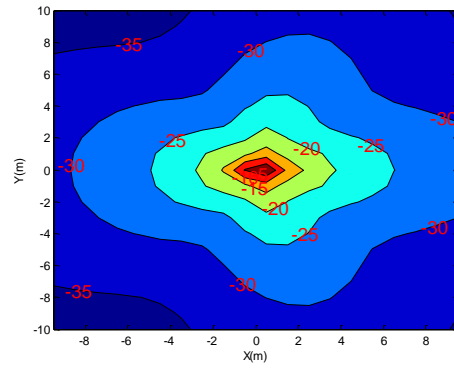
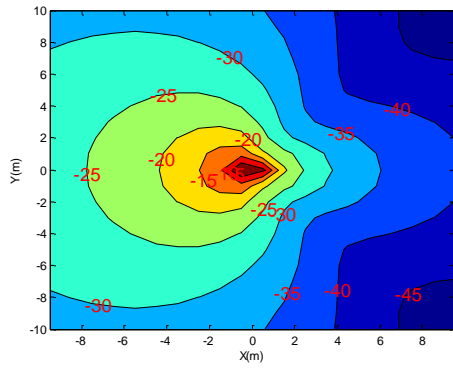
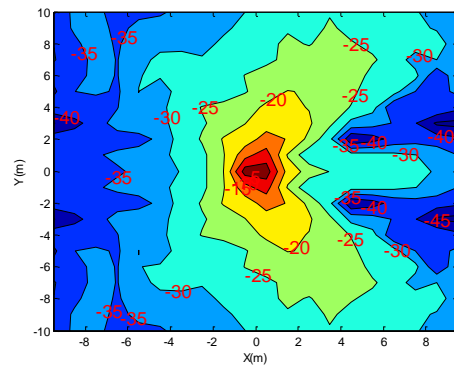
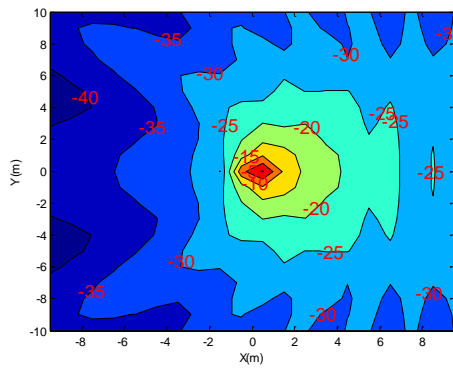


Fig. 2 Sketch map of the scattered radiation control with one error sensor and one control source

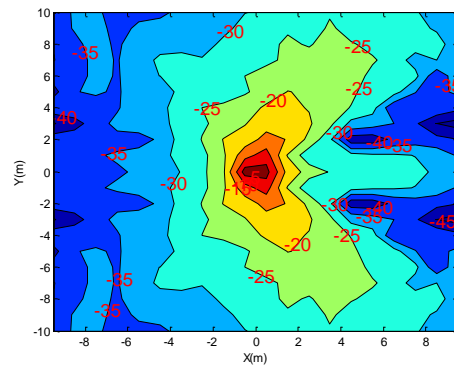
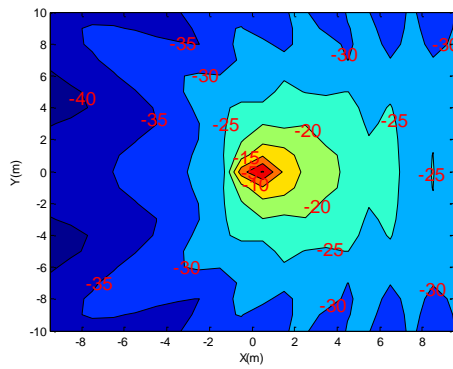
Fig. 3 (a) is the primary scattered sound field where an infinite reflected surface is located at $x=10\text{m}$. Shown in Fig. 3 (b) and (c), the active control for scattered radiation is still effective, due to the control source strengths calculated by Method 1 and Method 2 respectively. Although the function of the control system is to reduce the scattered sound pressure at the virtual error sensor, the area around the virtual error sensor also has the control effect. Taking the source (regarded as the active sonar) position as an example, it's about 10dB reduction of the scattered sound pressure level for 100Hz, and 7 dB reduction for 700Hz, shown in Fig. 3 (d).



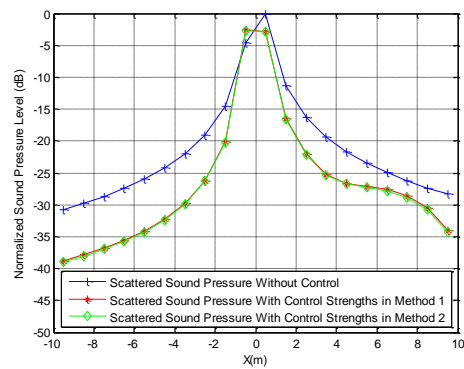
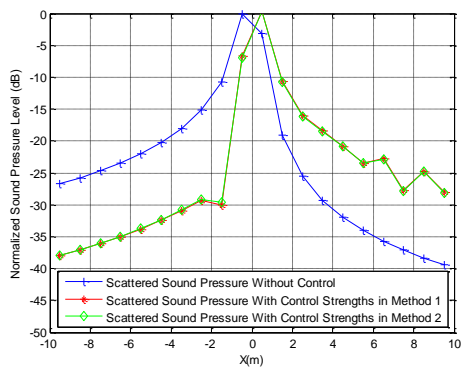
(a)



(b)



(c)



(d)

100Hz

700Hz

Fig. 3 Control effects by one-channel system at 100Hz (left line) and 700Hz (left line). The normalized sound pressure level of (a) the primary scattered field; (b) the controlled scattered

field by Method 1; (c) the controlled scattered field by Method 2; (d) the scattered sound field without and with control at x-axis.

It should be noted in Method 1, the first half elements in \mathbf{Q}_{opt} are usually not one by one equal to the bottom half part in \mathbf{Q}_{opt} , while the strengths of N_c control sources are chosen to be the first half elements in \mathbf{Q}_{opt} , thus the control effect at the error sensors will be degraded, compared with the optimum control source strengths in Method 2. But in other areas, it cannot be concluded that the control source strengths calculated by Method 2 is better than that by Method 1, shown in Fig.3.

4. CONCLUSIONS

In this paper, based on the mirror image principle in the sound field with an infinite reflected surface, two methods of calculating the control source strengths are proposed for the scattered radiation. Numerical simulations with one-channel control system are implemented to detect the control effect according to the two methods above. It is seen that the local active control is still effective, and although the control source strengths in Method 2 is optimum at the error sensors, it cannot be concluded that Method 2 is better than Method 1 in other areas.

5. ACKNOWLEDGEMENTS

Project supported by NSFC (No. 11874109) and the Fundamental Research Funds for the Central Universities (2242018k1G015 and 2242016k30013).

6. REFERENCES

1. T. B. A. Senior, "Control of the Acoustic Scattering Characteristics of a Rigid Sphere by Surface Loading", Journal of the Acoustical Society of America, 1965, 37(3):464-475.
2. X. Bao, V. K. Varadan, V. V. Varadan, et al, "Model of a bilaminar actuator for active acoustic control systems", Journal of the Acoustical Society of America, 1990, 87(3):1350-1352.
3. T. R. Howarth, V. K. Varadan, X. Bao, et al, "Piezocomposite coating for active underwater sound reduction", Journal of the Acoustical Society of America, 1992, 91(2):823-831.
4. T. R. Howarth, X. Bao, R. Moser, et al, "Digital time delay network for an active underwater acoustic coating", Journal of the Acoustical Society of America, 1993, 93(3):1613-1619.
5. L. D. Lafleur, F. D. Shields, J. E. Hendrix, "Acoustically active surfaces using piezorubber", Journal of the Acoustical Society of America, 1991, 90(3):1230-1237.
6. F. D. Shields, L. D. Lafleur, "Smart acoustically active surfaces", Journal of the Acoustical Society of America, 1998, 102(3):1559-1566.
7. R. D. Corsaro, B. Houston, J. A. Bucaro, "Sensor—actuator tile for underwater surface impedance control studies", Journal of the Acoustical Society of America, 1997, 102(3):1573-1581.
8. E. Friot, C. Bordier, "Real-time active suppression of scattered acoustic radiation", Journal of Sound & Vibration, 2004, 278(3):563-580.
9. E. Friot, A. Gintz, "Estimation and global control of noise reflections", Proceedings of Active 2009, Ottawa, Canada.

10. N. Han, X. Qiu, S. Feng, “*Active control of three-dimension impulsive scattered radiation based on a prediction method*”, *Mechanical Systems & Signal Processing*, 2012, 30:267-273.
11. J. Liu, X. Wang, M. Wu, et al, “*An active control strategy for the scattered sound field control of a rigid sphere*”, *Journal of the Acoustical Society of America*, 2018, 144(1):EL52-EL58.
12. X. Qiu, C. H. Hansen, X. Li, “*A comparison of near-field acoustic error sensing strategies for the active control of harmonic free field sound radiation*”, *Journal of Sound & Vibration*, 1998, 215(1):81-103.
13. J. J. Bowman, T. B. A. Senior, P. L. E. Uslenghi, “*Electromagnetic and Acoustic Scattering by Simple Shapes*”, North-Holland, Amsterdam, 1969.